Draft version January 25, 2022
Typeset using LaTeX default style in AASTeX631

The Kepler Problem

Kevin B. Moposita[1]

[1] *Villanova University*
800 Lancaster Avenue
Villanova, PA 19085, USA

1. INTRODUCTION

The purpose of this assignment is to evaluate the Kepler problem utilizing two methods: the Newton-Raphson iterative and Runge-Kutta methods. The Kepler problem, or the two-body problem, is meant to analyze the position of a small body's orbit with relation to a larger body. The Newton-Raphson iterative method is meant to be an analytical solution which utilizes many functions to quickly determine a true solution to non-linear equations. Unlike the Newton-Raphson method, the Runge-Kutta method is a numerical solution .With the two methods, the respective simulation of both orbits can be compared to determine points of deviation.

2. NEWTON-RAPHSON ITERATIVE METHOD

2.1. *Introduction*

The Newton-Raphson Iterative method starts off from Newton's Second Equation of Motion (equation 1) being substituted into Newton's Laws of Gravitation (equation 2) to create the equation necessary to determine the size of the two-body system's orbit (equation 3).

$$F = ma \tag{1}$$

$$F = -G\frac{m_1 m_2}{r^2}\frac{\overrightarrow{r}}{r} \tag{2}$$

$$\ddot{\overrightarrow{r}} = -\frac{GM}{r^2}\frac{\overrightarrow{r}}{r} \tag{3}$$

To plot one orbit of Halley's comet, the iterative solution will be used. The orbit would be constant and as accurate as can be. To utilize the iterative solution, the position that is within the calculated orbit will be iterated to the most approximate value that closely matches the actual value of the orbit. This is achieved with eccentric, mean, and true anomaly. Eccentric anomaly is the angle created by the position of the object within it's orbit and the origin point of the system. Mean anomaly measures the orbit's time in respect to it's period. True anomaly is the true value of the two-body's elliptical orbit. Mean anomaly is found first to then determine the eccentric anomaly, which is then utilized to calculate true anomaly.

2.1.1. *Mean Anomaly*

Mean anomaly is calculated first and the equation for it is below. M is the calculated mean anomaly, P is the period and t is time.

$$M = 2\pi\frac{tmodP}{P} \tag{4}$$

With this equation, the calculated orbit of Halley's comet will remain constant. As a result, present errors will be very minimal or non-existent.

2.1.2. *Eccentric Anomaly*

Eccentric anomaly can then be determined once the mean anomaly is calculated through the Newton-Raphson method. The Newton-Raphson method projects the object's position onto a circular orbit and then calculates it. To find the true value of the orbit, the position of the body's orbit is continuously iterated. The Newton-Raphson method is depicted through equation 5 and with the main function (equation 6), it was combined to equation 7 to calculate eccentric anomaly.

$$f(x_0) = f'(x_0)(x_0 - x_1) \tag{5}$$

$$M = E - esinE \tag{6}$$

$$E(n+1) = E_n - \frac{E_n - esinE_n - M}{1 - ecosE_n} \tag{7}$$

2.1.3. *True Anomaly*

With the calculated eccentric anomaly, true anomaly could now be calculated with equation 8.

$$tan\frac{\theta}{2} = \frac{1+e}{1-e}^{\frac{1}{2}} tan\frac{E}{2} \tag{8}$$

2.2. *Halley's Comet's Position*

Now true anomaly has now been determined, this allows for the calculation of the position of Halley's comet with respect to time.

3. NEWTON-RAPHSON METHOD RESULTS

The plots created of each anomaly can be found below. The plot of mean anomaly is depicted in *Figure 1*, eccentric anomaly is displayed on *Figure 2*, and true anomaly is depicted on *Figure 3*.

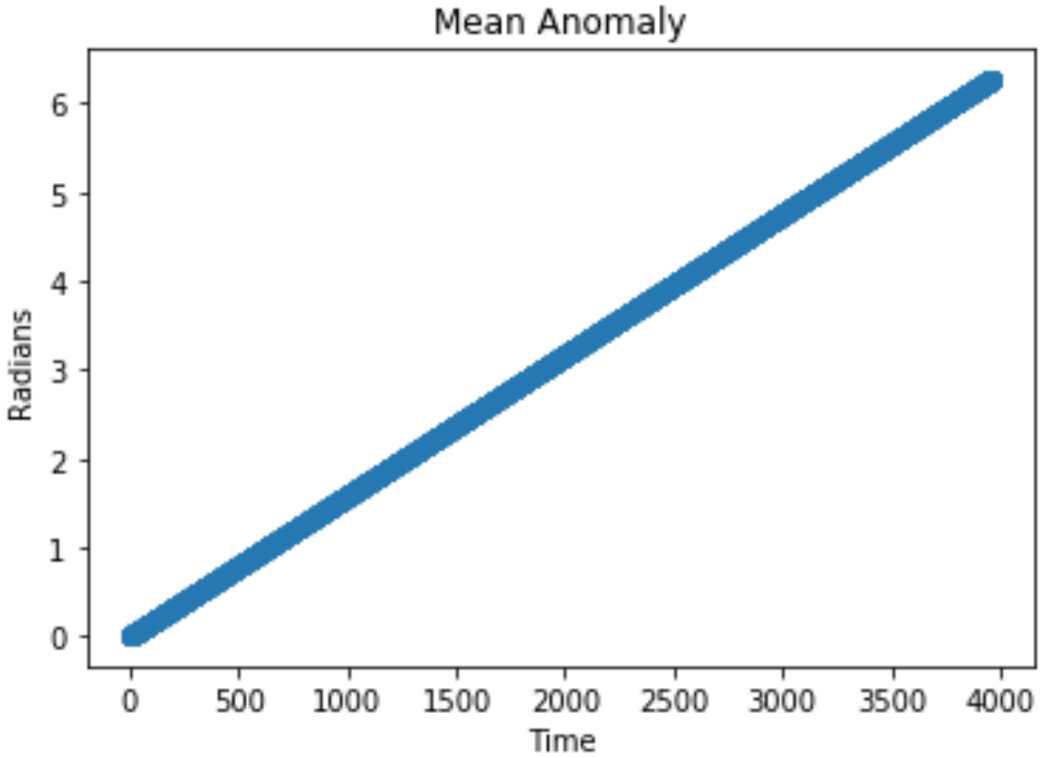

Figure 1. Figure 1 depicts the Mean Anomaly plot of Halley's comet.

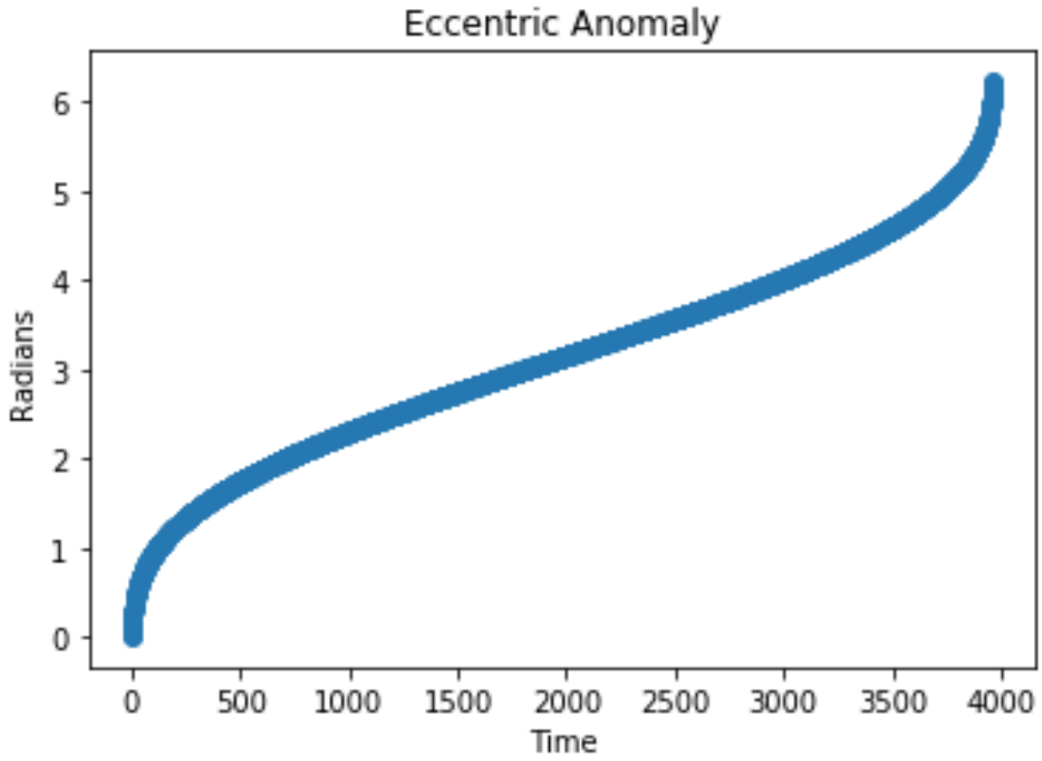

Figure 2. Figure 2 depicts the True Anomaly plot of Halley's comet.

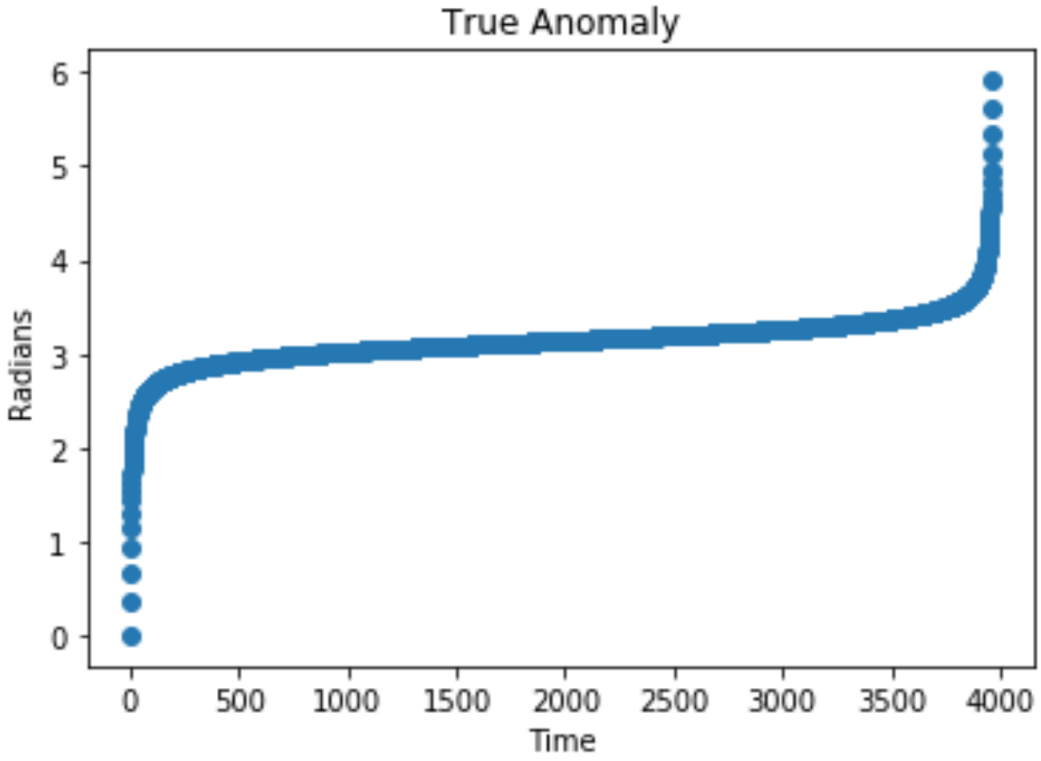

Figure 3. Figure 3 depicts True Anomaly of Halley's comet.

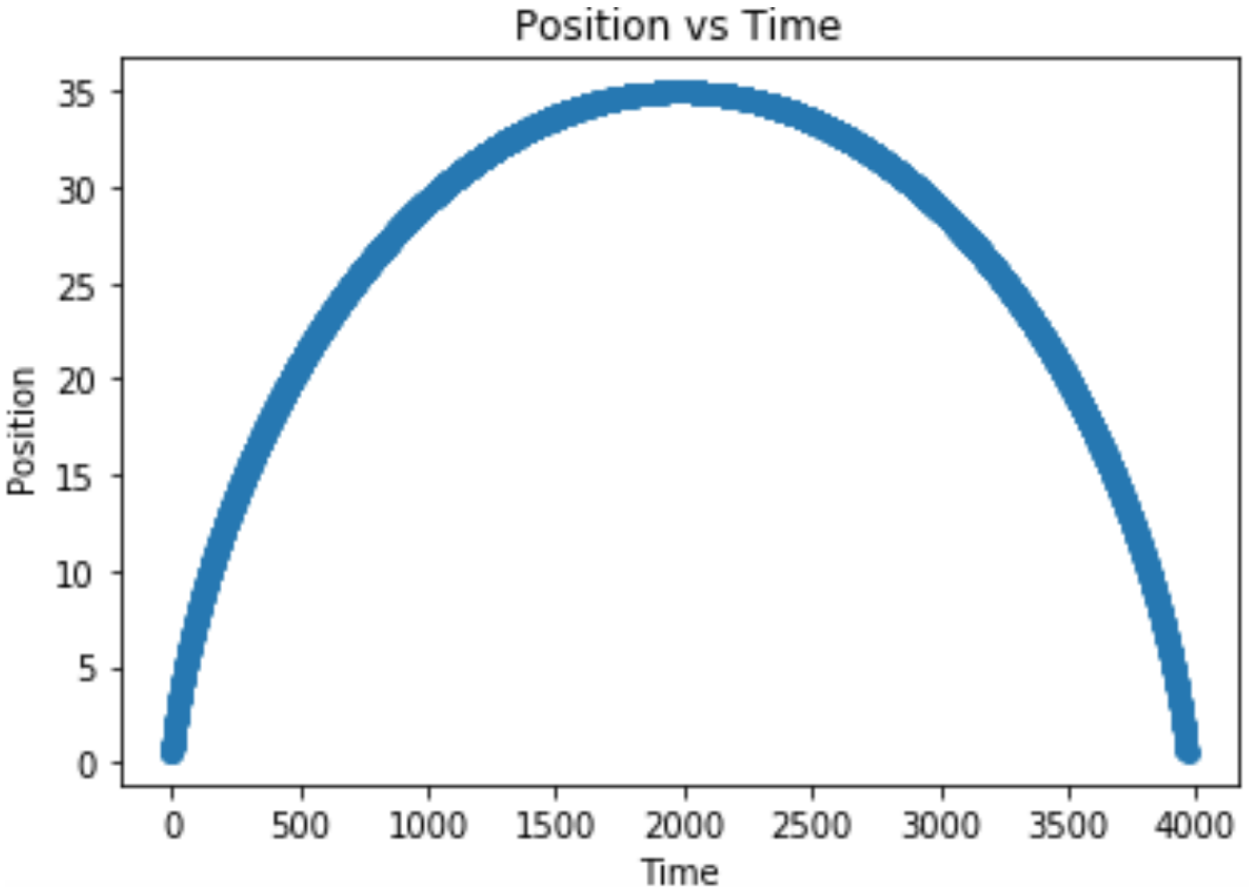

Figure 4. Figure 4 depicts the position of Halley's comet with respect to time.

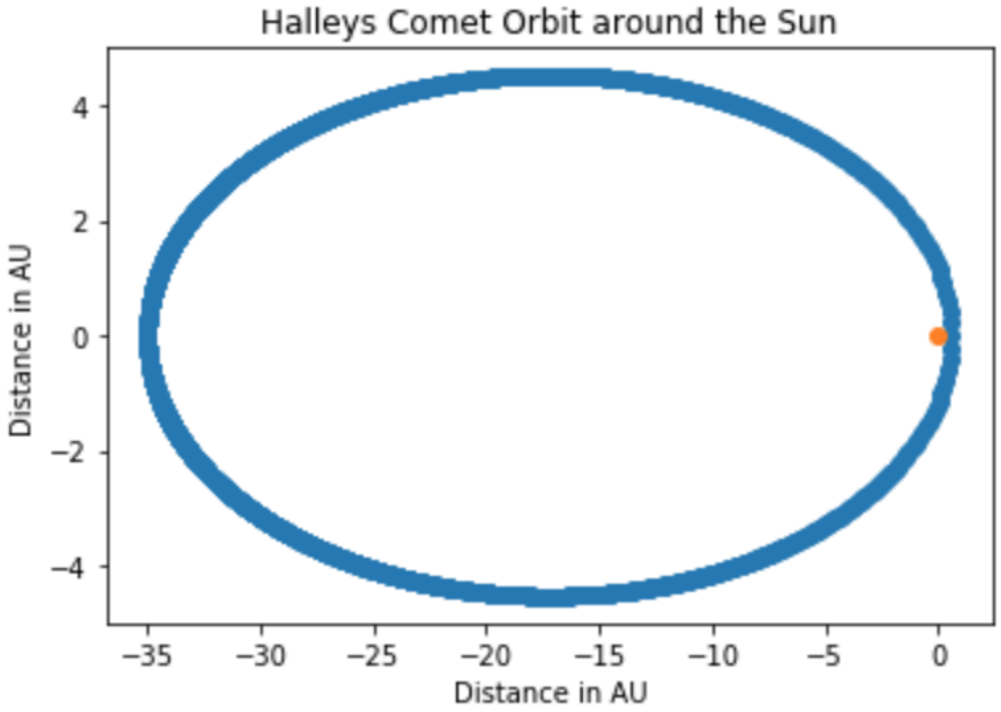

Figure 5. Figure 5 depicts the orbit of Halley's comet around the Sun, in orange.

3.1. *Additional Material*

In addition to the plots above, the orbit of Halley's comet was also plotted with respect to the orbits of all the planets within the solar system. *Figure 6* depicts all of the planets while *figure 7* depicts only the terrestrial planets. *Figure 8* also displays the comet's orbit with respect to the rest of the Solar System, but a polar plot. Eccentricity and periodic orbital values were obtained from Carroll and Ostlie (2017) to plot the planets' orbits.

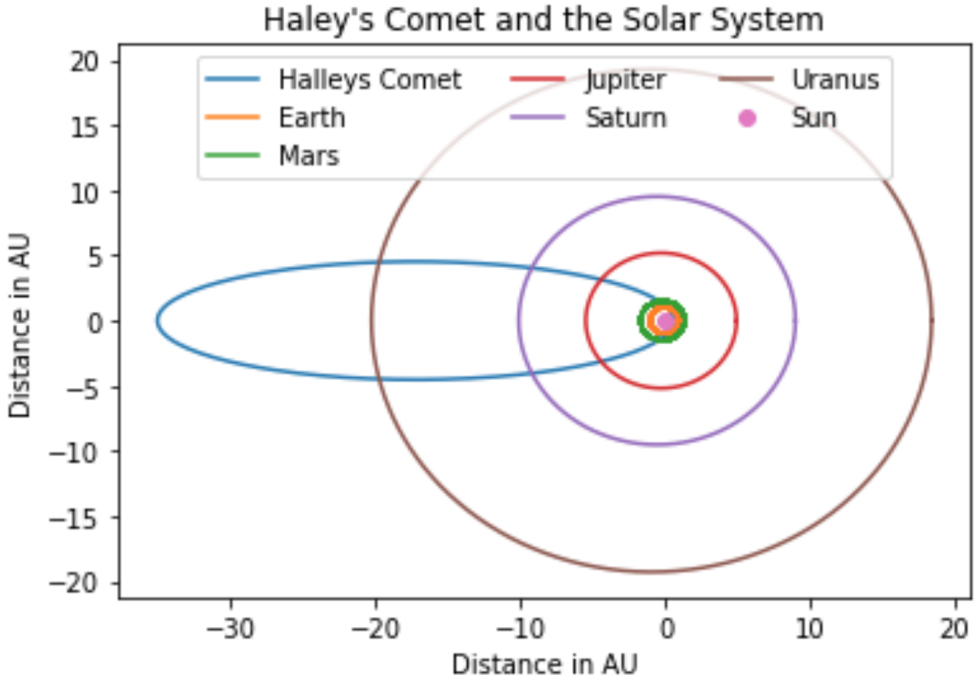

Figure 6. Figure 6 depicts the orbit of Halley's comet with respect to the orbits of the rest of the solar system.

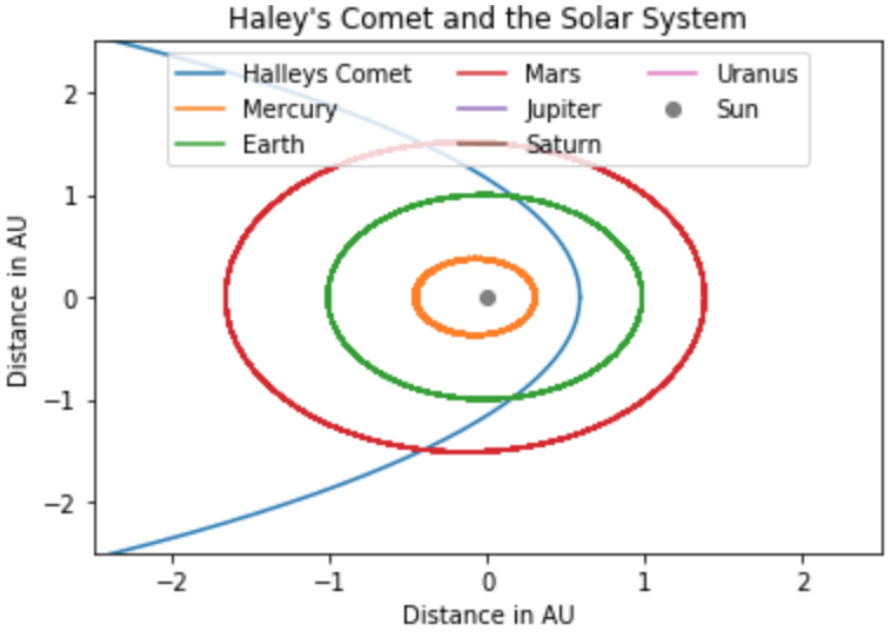

Figure 7. Figure 7 is a zoomed-in plot of the terrestrial planets and the orbit of Halley's comet.

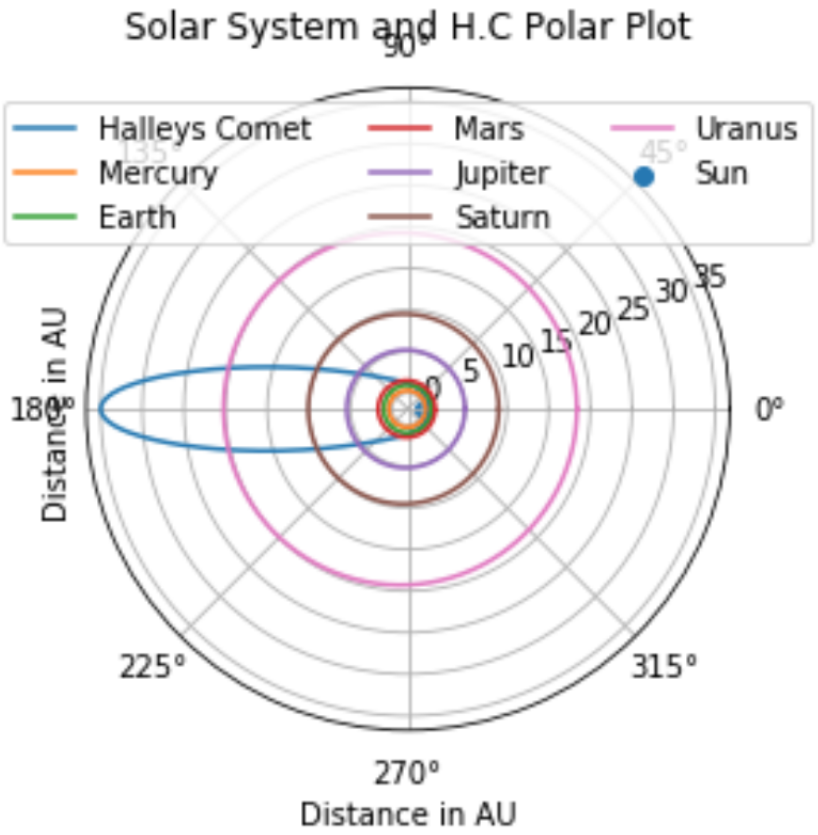

Figure 8. Polar plot of the solar system and Halley's comet.

4. RUNGE-KUTTA DERIVATION

Just like Newton-Raphson, the Runge-Kutta method can also model the orbit of a two-body system. However, unlike the Newton-Raphson method, the Runge-Kutta method creates an orbit that with time, begins to change and does not remain uniform. Before plotting this, it is critical to understand the Runge-Kutta approximation. To do so, the coefficients α_1, α_2, β_1, β_2, β_3, γ_1, γ_2, and γ_3 were computed for the third order Runge-Kutta expansion. The equations below were utilized to compute these coefficients and determining the solution for the third order.

$$y(x+h) = y(x) + \gamma_1 k_1 + \gamma_2 k_2 + \gamma_3 k_3 \tag{9}$$

$$k_1 = hf(x,y) \tag{10}$$

$$k_2 = hf(x+\alpha_1 h, y+\beta_1 k_1) \tag{11}$$

With the K_2 equation in hand, it can be Taylor expanded. The general Taylor expansion equation along with the expanded version of k_2 are below.

$$f(x+a,y+b) = f + af_x + bf_y + \frac{1}{2}(a^2 f_{xx} + abf_{xy} + abf_{yx} + b^2 f_{yy}) \tag{12}$$

$$k_2 = h[f + \alpha_1 h f_x + \beta_1 h f f_y + \frac{1}{2}(\alpha_1^2 h^2 f_{xx} + \alpha_1 h^2 \beta_1 f f_{xy} + \alpha_1 h^2 \beta_1 f f_{yx} + \beta_1^2 h^2 f^2 f_{yy})] \tag{13}$$

$$k_3 = hf(x+\alpha_2 h, y+\beta_2 k_1 + \beta_2 k_2) \tag{14}$$

$$\begin{aligned} k_3 = h[&f + \alpha_2 h f_x + \beta_2 h f f_y + \frac{1}{2}\alpha_2^2 h^2 f_{xx} + \frac{1}{2}\alpha_2 h^2 \beta_2 f f_{xy} + \frac{1}{2}\alpha_2 h^2 \beta_2 f f_{yx} + \frac{1}{2}\beta_2^2 h^2 f^2 f_{yy} + h\beta_3 f f_y \\ &+ h^2 \beta_3 \alpha_1 f_x f_y + h^2 \beta_1 \beta_3 f f_y^2 + \frac{1}{2}h^2 \alpha_2 \beta_3 f f_{xy} + h^2 \beta_2 \beta_3 f^2 f_{yy} + \frac{1}{2}h^2 \alpha_2 \beta_3 f f_{yx} + \frac{1}{2}h^2 \beta_3^2 f f_{yy}] \end{aligned} \tag{15}$$

$$\begin{aligned} y(x+h) = y(x) + h([&\gamma_1 + \gamma_2 + \gamma_3]f + h[\gamma_2\alpha_1 + \gamma_3\alpha_2]f_y + h[\gamma_2\beta_1 + \gamma_3\beta_2 + \gamma_3\beta_3]f f_y + \frac{1}{2}h^2[\gamma_2\alpha_1^2 + \gamma_3\alpha_1^2]f_{xx} \\ &+ \frac{1}{2}h^2[\gamma_2\alpha_1\beta_1 + \gamma_3\alpha_2\beta_2 + \gamma_3\alpha_2\beta_3]f f_{xy} + \frac{1}{2}h^2[\gamma_2\alpha_1\beta_1 +_3 \alpha_2\beta_2 + \gamma_3\alpha_2\beta_3]f f_{yy} \\ &+ h^2[\gamma_3\alpha_1\beta_3]f_x f_y + h^2[\gamma_3\beta_1\beta_3]f f_y^2 + h^2[\frac{1}{2}\gamma_2\beta_1^2 + \frac{1}{2}\gamma_3\beta_2^2 + \gamma_3\beta_2\beta_3 + \frac{1}{2}\beta_3^2]f^2 f_{yy}) \end{aligned} \tag{16}$$

With k_3 expanded, the coefficients mentioned earlier can now be determined.

$$\gamma_1 + \gamma_2 + \gamma_3 = 1 \tag{17}$$

$$\gamma_2\alpha_1 + \gamma_3\alpha_2 = \frac{1}{2} \tag{18}$$

$$\gamma_2\beta_1 + \gamma_3(\beta_2 + \beta_3) = \frac{1}{2} \tag{19}$$

$$\gamma_2\alpha_1^2 + \gamma_3\alpha_2^2 = \frac{1}{3} \tag{20}$$

This next equation was calculated twice and as a result, will only be displayed once.

$$\gamma_2\alpha_1\beta_1 + \gamma_3\alpha_2(\beta_2 + \beta_3) = \frac{1}{3} \tag{21}$$

$$\gamma_3\alpha_1\beta_3 = \frac{1}{6} \tag{22}$$

$$\gamma_3\beta_1\beta_3 = \frac{1}{6} \tag{23}$$

$$\gamma_2\beta_1^2 + \gamma_3(\beta_2 + \beta_3)^2 = \frac{1}{3} \tag{24}$$

With these relationships in hand, the coefficients mentioned can now be solved. Utilizing Runge-Kutta's third order method, the following values can be considered as correct conditions as determined by Butcher (1996).

$$\alpha_1 = \frac{1}{2} \tag{25}$$

$$\alpha_2 = 1 \tag{26}$$

$$\beta_1 = \frac{1}{2} \tag{27}$$

$$\beta_2 = -1 \tag{28}$$

$$\beta_3 = 2 \tag{29}$$

$$\gamma_1 = \frac{1}{6} \tag{30}$$

$$\gamma_2 = \frac{2}{3} \tag{31}$$

$$\gamma_3 = \frac{1}{6} \tag{32}$$

5. RUNGE-KUTTA 4TH ORDER DIFFERENTIAL SOLUTION

This section of the assignment required the usage of Runge-Kutta's 4th order method. *Figure 9* is the resulting plot of the comet's orbit as determined by the Runge-Kutta 4th order method. As displayed, the orbit itself is a close approximation to the calculated orbit the iterative method produced.

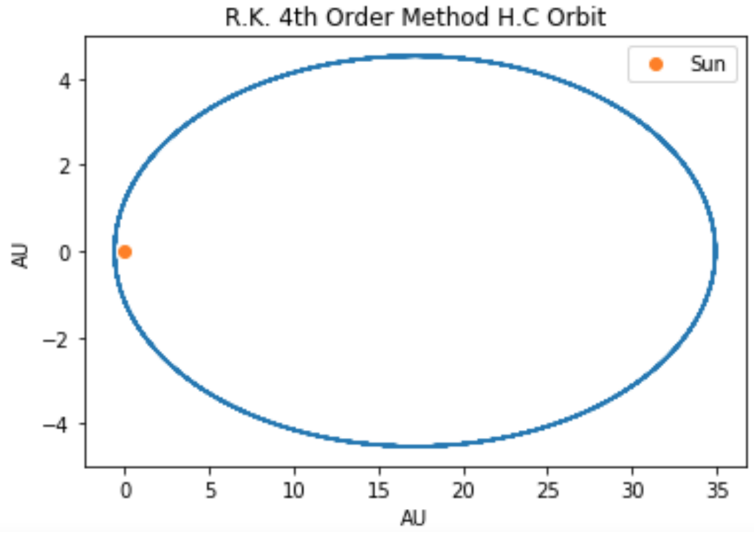

Figure 9. Runge-Kutta's 4th Order Method was utilized to plot the orbit of Halley's comet with reference to the Sun.

Taking it a step further, this number of orbits was increased to 1000 and plotted. This is depicted on *Figure 10*. As it can be observed, the comet's orbit begins to precess at aphelion. This change in the orbit is best analyzed through *Figure 11* and *figure 12*. *Figure 11* measures the distance from aphelion against the number of orbits. As displayed, as the number of orbits increases, the distance at aphelion is steadily decreasing. *Figure 12* measures the error between the iterative and Runge-Kutta methods against the number of orbits. In agreement with the previous plot, the percent error between both methods steadily rises as the number of orbits increases.

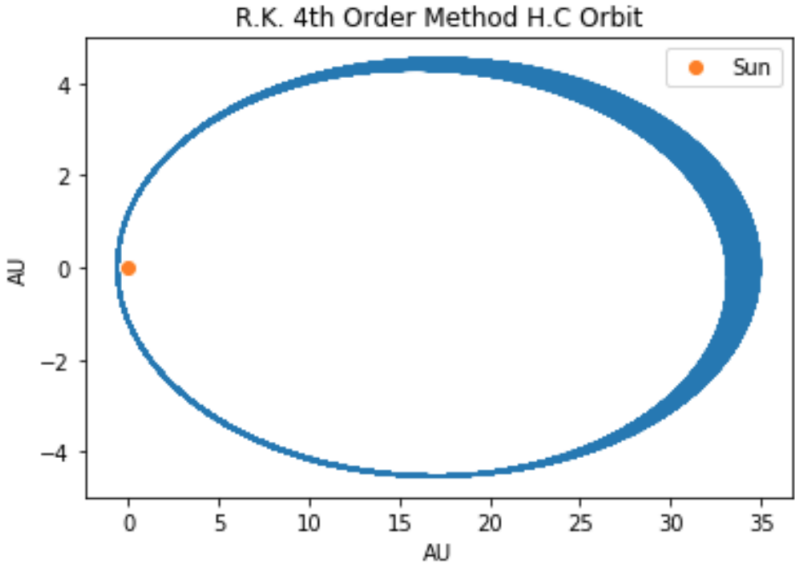

Figure 10. Runge-Kutta 4th Order orbit of H.C. with 1000 orbits.

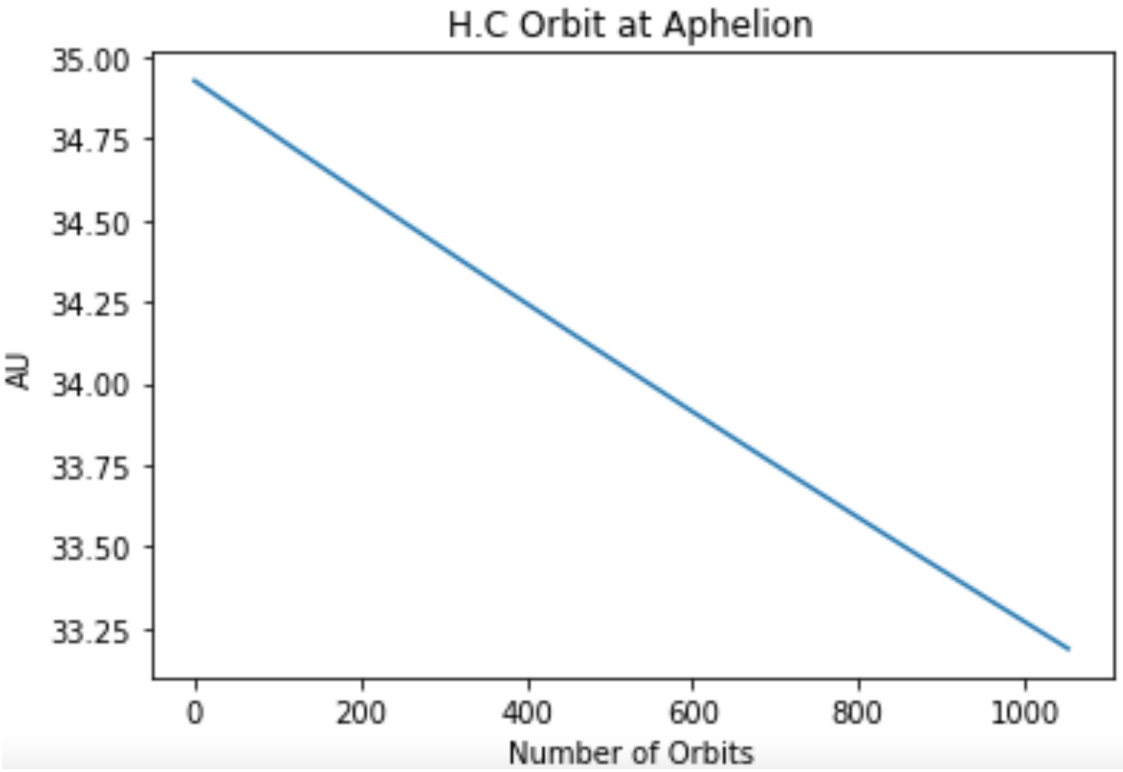

Figure 11. Depiction of H.C's distance at aphelion changing with the number of orbits.

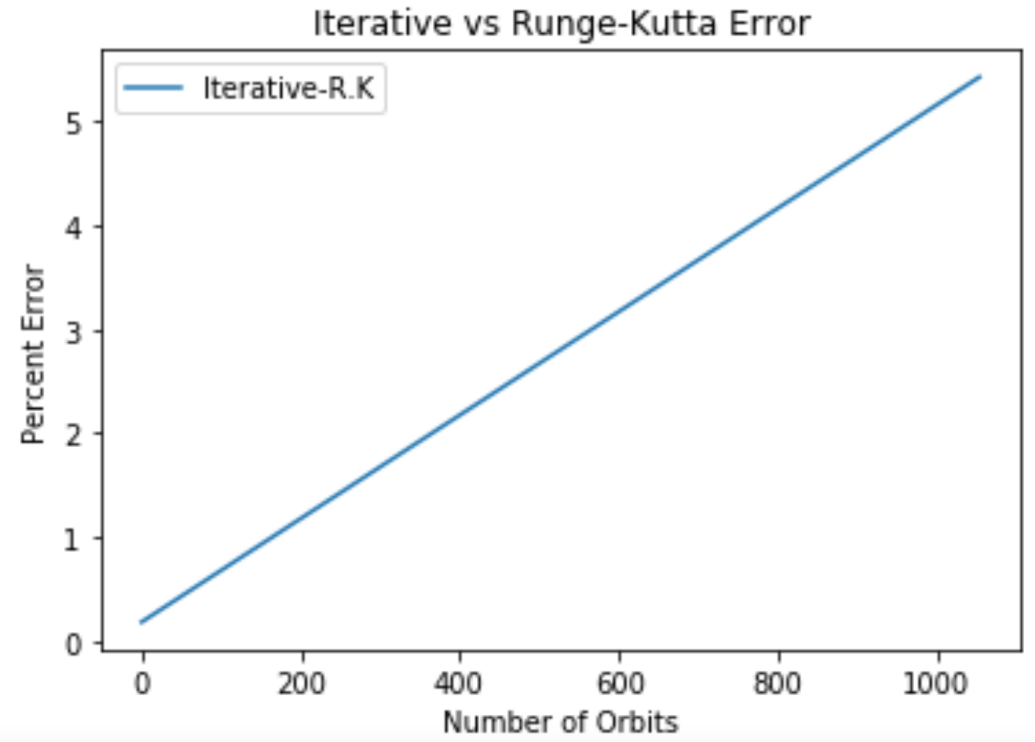

Figure 12. Depiction of the error associated with the Runge-Kutta method compared to Newton's method.

6. STABILITY

This section of the assignment aimed to analyze the orbit of Halley's comet under different differential integrators. *Figure 13* compares the projected orbit of Halley's comet under the iterative and Runge-Kutta methods. As can be noticed in the plot, the Runge-Kutta orbit suffers from precession near the top right-hand side and the lower right-hand side.

Besides the iterative and Runge-Kutta methods, another differential integrator that can model the orbit is Euler's method, once initial conditions are provided. Once plotted, the difference between Euler's method and the other two is very much apparent. *Figure 14* displays all three methods projected onto one plot. Before the number of orbits begins to increase, the initial shape of the comet's orbit is vastly larger and the position is also vastly offset from the general position of the iterative and Runge-Kutta versions of the orbit. These errors can be attributed to the fact that Euler's method is best utilized for circular orbits, whereas Halley's comet has an elliptical orbit.

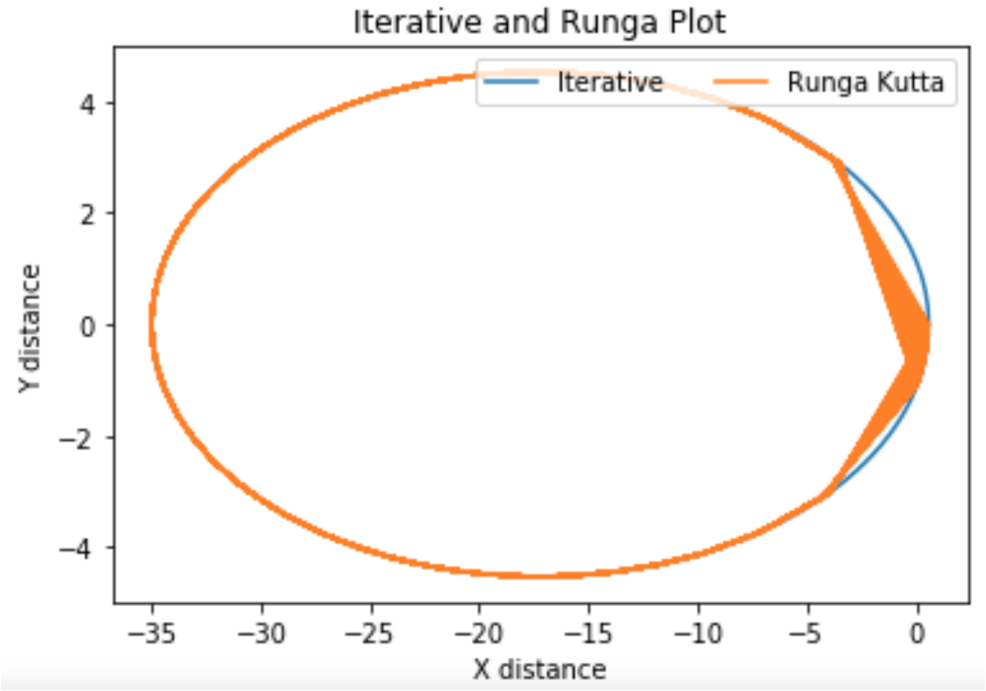

Figure 13. Plot depiction of the stability of H.C.'s orbit through the iterative and Runge-Kutta methods. Runge-Kutta's plot shows a clear precession on the top right-hand side of its orbit.

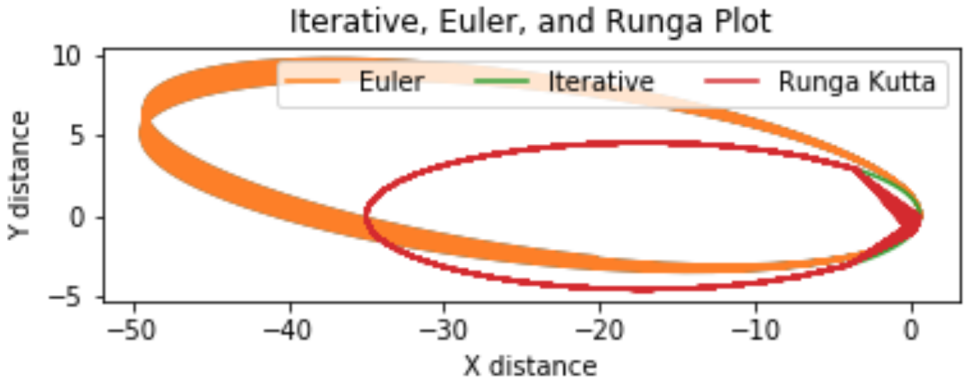

Figure 14. Depiction of the orbit of Halley's comet utilizing the iterative, Runge-Kutta, and Euler methods.

7. CONCLUSION

As this paper shows, there are various methods that can be utilized to solve the two-body problem or Kepler's problem. Although the Newton-Raphson method proves to be the most accurate of them all, Runge-Kutta also provides a fairly close approximation to the orbital value, which in this case, was for the orbit of Halley's comet. Euler's method was also utilized, but displays a large margin of error due to its limitation to circular orbits. As a result,the Newton-Raphson and Runge-Kutta methods are the best choices in terms of modeling this orbit.

REFERENCES

Butcher, J. (1996). A history of runge-kutta methods. *Applied Numerical Mathematics*, 20(3):247–260.

Carroll, B. W. and Ostlie, D. A. (2017). *An Introduction to Modern Astrophysics, Second Edition*. Cambridge University Press.